Available online at www.sciencedirect.com
SCIENCE DIRECT®
Thermochimica Acta 406 (2003) 77–87
thermochimica acta
www.elsevier.com/locate/tca

Thermal kinetic TG-analysis of metal oxalate complexes

Li Jun*, Zhang Feng-Xing, Ren Yan-Wei, Hun Yong-Qian, Nan Ye-Fei

Department of Chemistry, Northwest University, Key Laboratory of Physicoinorganic Chemistry, TaiBai Road 229, Xi'an 710069, Shaanxi Province, PR China

Received 19 September 2002; received in revised form 25 March 2003; accepted 3 April 2003

Abstract

The TG/DSC curves of $K_3[Cr(C_2O_4)_3]\cdot 3H_2O$, $K_3[Al(C_2O_4)_3]\cdot 3H_2O$, $K_3[Fe(C_2O_4)_3]\cdot 3H_2O$ and $K_2[Cu(C_2O_4)_2]\cdot 2H_2O$ in nitrogen were determined at the heating rate of 15, 10, 5, and 2 °C min^{-1}, respectively. A non-linear optimization was applied for different reaction models to perform single and overall steps optimizations. Kinetic parameters were given, and the most probable mechanism functions were suggested.

Keywords: Thermal analysis; Kinetic; Metal oxalate complexes

1. Introduction

$C_2O_4^{2-}$ is a good ligand and can be coordinated with many transition and non-transition metals. Their thermal decomposition processes are relatively complicated because of the reduction property of $C_2O_4^{2-}$. So their thermal analysis studies are often in attention. A review on the thermal decomposition of some solid oxalates has been given by Harris and co-workers [1]. The kinetics and mechanisms of thermal decomposition of solids have been reviewed by L'vov [2]. The thermal decomposition of the type $K_3[M(C_2O_4)_3]\cdot 3H_2O$ (where M = Co, Cr, Fe, Ga) and $K_2[Cu(C_2O_4)_2]\cdot 2H_2O$ (where M = Cu, Zn, Pd, Pt) were studied [3–11]. Recently, we also studied the thermal decomposition of $K_3[Cr(C_2O_4)_3]\cdot 3H_2O$, $K_3[Al(C_2O_4)_3]\cdot 3H_2O$, $K_3[Fe(C_2O_4)_3]\cdot 3H_2O$ and $K_2[Cu(C_2O_4)_2]\cdot 2H_2O$ in nitrogen, and obtained E_a, $\lg A$ of each steps by means of Ozawa–Flynn–Wall, Friedman and ASTME698 methods [12]. But the kinetic studies of the type $K_3[M(C_2O_4)_3]\cdot 3H_2O$ and $K_2[Cu(C_2O_4)_2]\cdot 2H_2O$ are rarely reported until now. In this article, a non-linear optimization was applied for different reaction models to perform single and overall steps optimizations and kinetic parameters were given, the most probable mechanism functions were suggested for the complexes of $K_3[Cr(C_2O_4)_3]\cdot 3H_2O$, $K_3[Al(C_2O_4)_3]\cdot 3H_2O$, $K_3[Fe(C_2O_4)_3]\cdot 3H_2O$ and $K_2[Cu(C_2O_4)_2]\cdot 2H_2O$.

2. Experimental

2.1. Reagents

$K_2C_2O_4\cdot H_2O$, $H_2C_2O_4\cdot 2H_2O$, $K_2Cr_2O_7$, $Al_2(SO_4)_3$, $FeCl_3\cdot 6H_2O$ and $CuSO_4\cdot 5H_2O$ are all A.R. or G.R. from China.

* Corresponding author.
E-mail address: junli@nwu.edu.cn (L. Jun).

0040-6031/$ – see front matter © 2003 Elsevier B.V. All rights reserved.
doi:10.1016/S0040-6031(03)00221-1

Table 1
The selective 15 mechanism functions for evaluation of the kinetic equations

Name of functions	Kinetics mechanisms	Form of functions		Symbol
		$f(\alpha)$	$G(\alpha)$	
First order		$(1-\alpha)$		F1
Second order	Formal chemical reaction	$(1-\alpha)^2$	$(1-\alpha)^{-1}$	F2
*N*th order		$(1-\alpha)^n$	$[1-(1-\alpha)^{1-n}]/(1-n)$	Fn
Parabola law	One-dimensional diffusion	$0.5\alpha^{-1}$	α^2	D1
Valensi equation	Two-dimensional diffusion	$-1/\ln(1-\alpha)$	$\alpha+(1-\alpha)\ln(1-\alpha)$	D2
Jander equation	Three-dimensional diffusion	$1.5(1-\alpha)^{2/3}[1-(1-\alpha)^{1/3}]^{-1}$	$[1-(1-\alpha)^{1/3}]^2$	D3
Ginstling–Brounshtein	Three-dimensional diffusion	$1.5[(1-\alpha)^{-1/3}-1]^{-1}$	$((1-2\alpha)/3)-(1-\alpha)^{2/3}$	D4
Contracting sphere				
Cylindrical symmetry	Phase boundary reaction	$2(1-\alpha)^{1/2}$	$1-(1-\alpha)^{1/2}$	R2
Spherical symmetry	Phase boundary reaction	$3(1-\alpha)^{2/3}$	$1-(1-\alpha)^{1/3}$	R3
Prout–Tompkins equation		$(1-\alpha)\alpha$	$\ln[\alpha/(1-\alpha)]$	B1
Expanded Prout–Tompkins equation	Auto-catalysis, Ramiform nucleation	$(1-\alpha)^n\alpha^a$		Bna
		$(1-\alpha)(1+K\alpha)$		C1
Avrami–Erofeev equation	Two-dimensional nucleation and growth	$(1-\alpha)[-\ln(1-\alpha)]^{1/2}$	$[-\ln(1-\alpha)]^{1/2}$	A2
	Three-dimensional nucleation and growth	$3(1-\alpha)[-\ln(1-\alpha)]^{2/3}$	$[-\ln(1-\alpha)]^{1/3}$	A3
	N-Dimensional nucleation and growth	$n(1-\alpha)[-\ln(1-\alpha)]^{(n-1)/n}$	$[-\ln(1-\alpha)]^{1/n}$	An

2.2. Preparation

$K_3[Al(C_2O_4)_3]\cdot 3H_2O$, $K_3[Cr(C_2O_4)_3]\cdot 3H_2O$, $K_3[Fe(C_2O_4)_3]\cdot 3H_2O$ and $K_2[Cu(C_2O_4)_2]\cdot 2H_2O$ were prepared according to the literature [13].

2.3. Thermal analysis

NETZSCH STA449C thermal analysis instrument (made in Germany). An alumina crucible container was used in nitrogen. The rate of heating was 15, 10, 5, and 2 °C min^{-1}, and sensitive of the instrument is 0.1 μg. The sample mass is 3–6 mg.

2.4. The theory base of the kinetics estimation of the thermal decomposition

According to non-isothermal kinetic models, the kinetic equation of solid thermal decomposition is given as follows:

$$\frac{d\alpha}{dT} = \frac{A}{\beta} f(\alpha)\exp\left(\frac{-E_a}{RT}\right) \quad (1)$$

where α is fractional extent of reaction in time t, β the heating rate, E_a the activation energy, A the pre-exponential factor, and $f(\alpha)$ is kinetic differential function. Its integral form is as follows:

$$G(\alpha)\int_0^\alpha \frac{d\alpha}{f(\alpha)} = \frac{A}{\beta}\int_0^T \exp\left(\frac{-E_a}{RT}\right) dT \quad (2)$$

Fifteen mechanism functions in Table 1 were used to fit kinetics curves. The kinetics software from NETZSCH was adopted.

3. Results and discussion

3.1. Thermal decomposition processes

The thermal decomposition processes of $K_3[Al(C_2O_4)_3]\cdot 3H_2O$, $K_3[Cr(C_2O_4)_3]\cdot 3H_2O$, $K_3[Fe(C_2O_4)_3]\cdot 3H_2O$ and $K_2[Cu(C_2O_4)_2]\cdot 2H_2O$ have been reported previously by [12]. There, some data were given in Table 2.

Table 2
The thermal decomposition processes of the complexes $K_3M(C_2O_4)_3{\cdot}3H_2O$ (M = Al, Cr, Fe) and $K_2Cu(C_2O_4)_2{\cdot}2H_2O$

Steps	$K_3Al(C_2O_4)_3{\cdot}3H_2O$	$K_3Cr(C_2O_4)_3{\cdot}3H_2O$	$K_3Fe(C_2O_4)_3{\cdot}3H_2O$	$K_2[Cu(C_2O_4)_2]{\cdot}2H_2O$
I	$\downarrow -3H_2O$ $K_3Al(C_2O_4)_3$	$\downarrow -3H_2O$ $K_3Cr(C_2O_4)_3$	$\downarrow -3H_2O$ $K_3Fe(C_2O_4)_3$	$\downarrow -2H_2O$ $K_2[Cu(C_2O_4)_2]$
II	$\downarrow -1/2(3CO_2 + 6CO)$ $1/2Al_2O_3 + 3/2K_2CO_3$	$\downarrow -1/10(16CO + 9CO_2)$ $3/2K_2C_2O_4 + 1/5(Cr_3O_4 + Cr_2(CO_3)_3$	$\downarrow -(CO_2 + 1/2CO)$ $1/2K_2CO_3 + K_2[FeC_2O_4]_2$	$\downarrow -(3/2CO_2 + 1/2CO)$ $1/2Cu_2O + K_2C_2O_4$
II		$\downarrow -1/30(37CO + 23CO_2)$ $3/2K_2CO_3 + 1/3Cr_3O_4$	$\downarrow -5/2CO$ $3/2K_2CO_3 + FeCO_3$	$\downarrow -CO$ $K_2CO_3 + 1/2Cu_2O$
IV			$\downarrow CO_2 + 1/6O_2$ $3/2K_2CO_3 + 1/6Fe_3O_4 + 1/2Fe$	

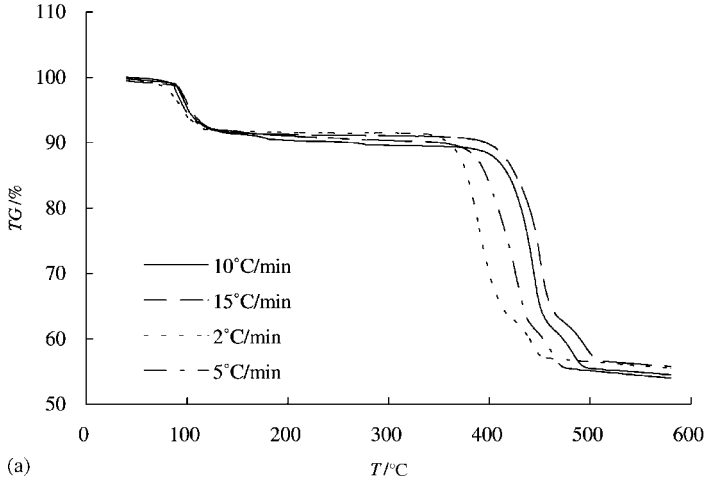

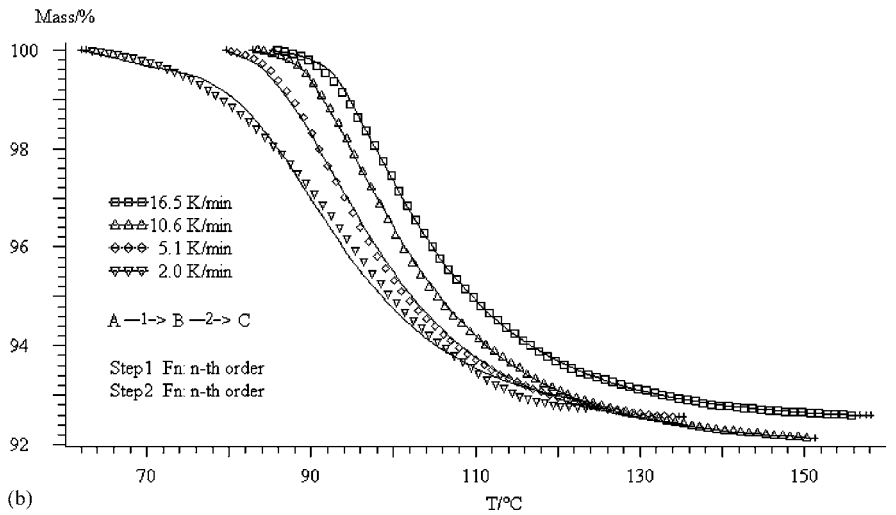

Fig. 1. The TG curve of $K_3Al(C_2O_4)_3{\cdot}3H_2O$ at the heating rate of 15, 10, 5, and 2 °C min^{-1}, respectively (a); the first step (b) and the second step (c) were the best fit to mechanism functions. The solid line is the fit curve.

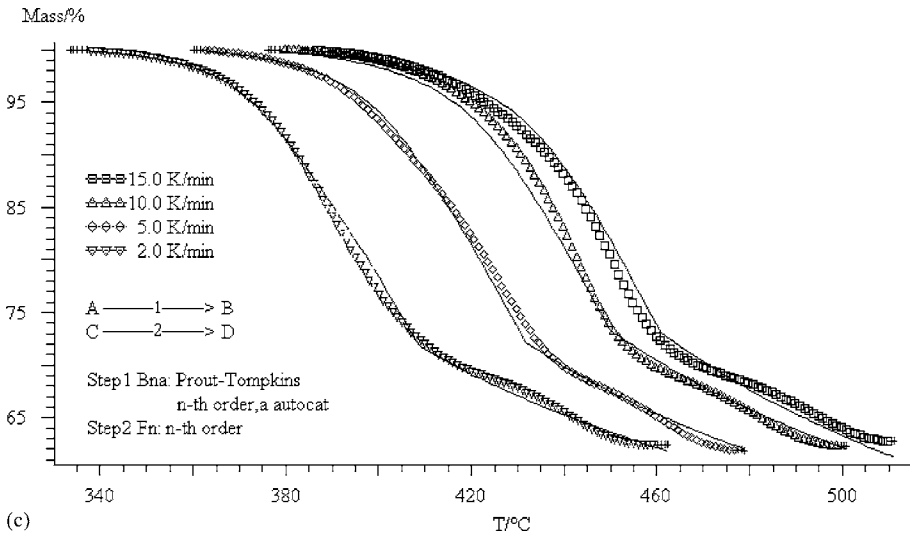

Fig. 1. (*Continued*).

Table 3
The optimized mechanism functions and kinetics parameters of $K_3M(C_2O_4)_3{\cdot}3H_2O$ (M = Cr, Fe, Al) and $K_2Cu(C_2O_4)_2{\cdot}2H_2O$

Complexes	Steps	Mechanism	E_a (kJ mol^{-1})	lg$A$ (s^{-1})	Reaction order n	Exponent a	Correction coefficient
$K_3[Al(C_2O_4)_3]{\cdot}3H_2O$	I	Fn	88.56	11.39	0.36		0.99944
		Fn	227.49	30.54	3.65		
	II	Bna	107.03	6.15	21.68	0.82	0.99861
		Fn	150.49	8.72	8.91E−02		
$K_3[Cr(C_2O_4)_3]{\cdot}3H_2O$	I	Fn	81.87	9.94	2.57		0.99816
	II	Bna	297.71	18.78	0.60	0.18	0.99943
	III	Fn	361.78	16.02	0.78		0.99856
$K_3[Fe(C_2O_4)_3]{\cdot}3H_2O$	I	Bna	63.67	8.13	1.20	0.23	0.99846
		Bna	79.51	9.78	1.54	0.81	
	II	Fn	60.90	3.08	0.19		0.99888
		Bna	99.80	8.08	1.14	0.84	
	III	R3	344.00	23.25			0.99834
		Bna	168.42	12.32	20.66	1.34	
	IV	Fn	194.39	11.07	0.89		0.99978
		Fn	185.25	9.66	0.75		
$K_2[Cu(C_2O_4)_2]{\cdot}2H_2O$	I	Bna	193.52	26.48	2.06	0.56	0.99988
		Bna	72.02	8.59	0.65	0.65	
	II	A3	190.51	15.82			0.99961
		D3	390.12	35.85			

3.2. Thermal kinetic TG-analysis of $K_3[Al(C_2O_4)_3]\cdot 3H_2O$

TG kinetic of $K_3[Al(C_2O_4)_3]\cdot 3H_2O$ were analyzed. The TG data for the first step and second step of $K_3[Al(C_2O_4)_3]\cdot 3H_2O$ were non-line fit to 15 mechanism functions which were given in Table 1. Single reaction mechanism was tried to fit, but it do not fit good. So, we base the change of activation energy with the reacted fraction α, and try to use multireaction mechanisms to fit. The results were satisfied (Fig. 1).

From Table 3, we see that the dehydration of $K_3[Al(C_2O_4)_3]\cdot 3H_2O$ adopted the A → B → C sequential reaction, and the reaction mechanism was Fn–Fn. The activation energy of the later was larger than the former; the second step adopted A → B and

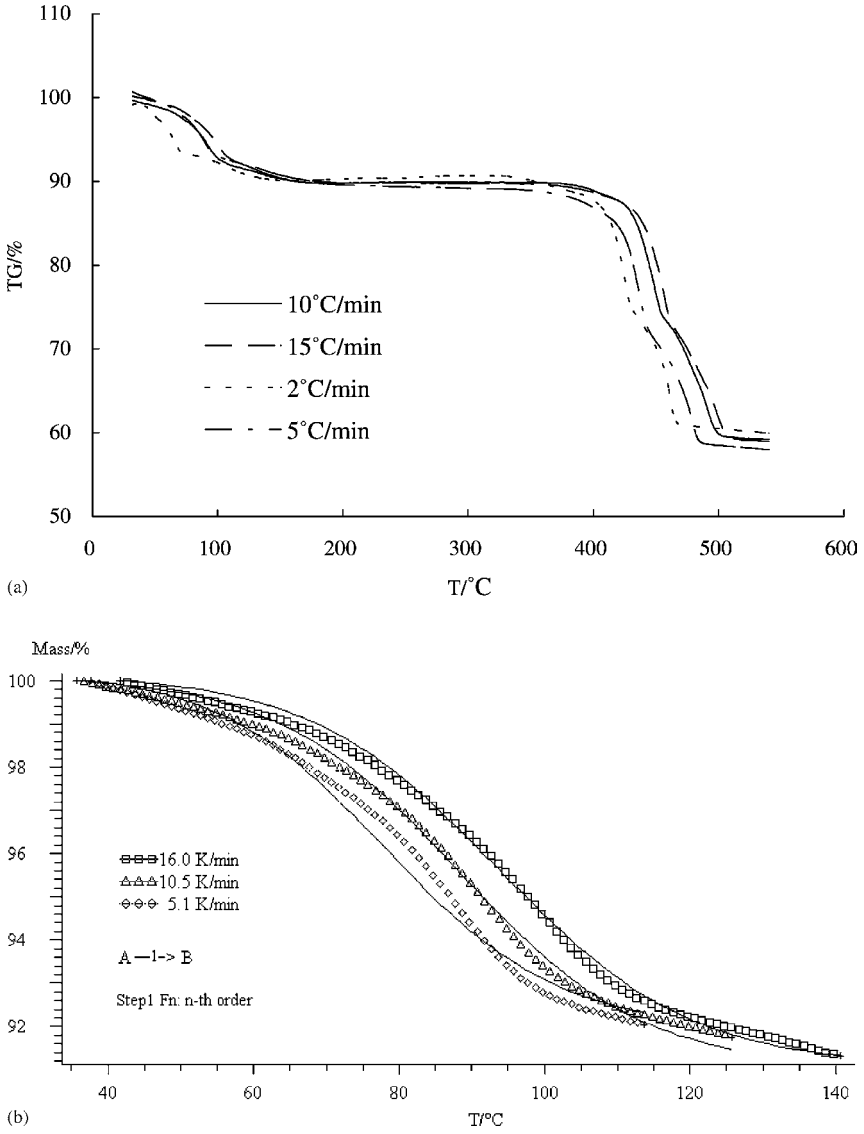

Fig. 2. The TG curve of $K_3Cr(C_2O_4)_3\cdot 3H_2O$ at the heating rate of 15, 10, 5, and 2 °C min^{-1}, respectively (a); the first step (b), the second step (c) and the third step (d) were the best fit to mechanism functions. The solid line is the fit curve.

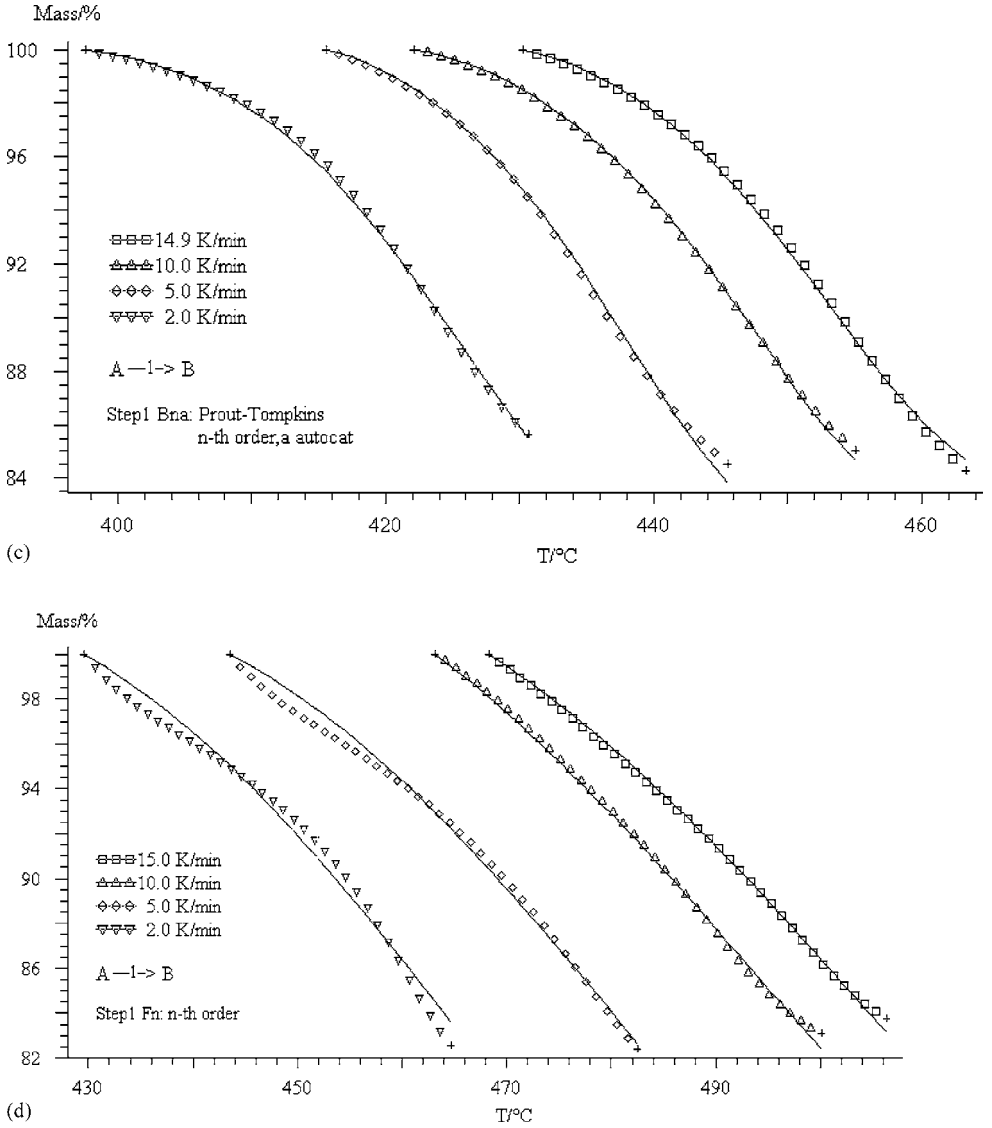

Fig. 2. (*Continued*).

C → D reaction mode, and the reaction mechanism was Bna–Fn.

3.3. Thermal kinetic TG-analysis of $K_3[Cr(C_2O_4)_3]\cdot 3H_2O$

TG kinetic of three steps of $K_3[Cr(C_2O_4)_3]\cdot 3H_2O$ were analyzed, respectively, and each step was non-line fit to 15 mechanism functions which were given in Table 1. The multireaction mechanism was tried to fit, but it does not fit good. This demonstrated that three steps of $K_3[Cr(C_2O_4)_3]\cdot 3H_2O$ were a single reaction mechanism. So single reaction mechanism was used, and the results were shown in Fig. 2 and Table 3.

The optimized mechanism functions of the three steps were Fn, Bna and Fn, respectively. Relevant E_a were 77.79, 284.16, and 261.25 kJ mol^{-1}, and $\lg A$ were 9.468, 18.78, and 16.02 s^{-1}. Compared with optimized multireaction mechanism of

$K_3[Al(C_2O_4)_3]\cdot 3H_2O$, the correction coefficient of single reaction mechanism was not so good.

3.4. Thermal kinetic TG-analysis of $K_3[Fe(C_2O_4)_3]\cdot 3H_2O$

Similarly, TG kinetic of four steps of $K_3[Fe(C_2O_4)_3]\cdot 3H_2O$ were also analyzed, respectively, and each step was non-line fit to 15 mechanism functions which were given in Table 1. Single reaction mechanism was tried to fit, but it does not fit good. So multireaction mechanism was used, and the results were shown in Fig. 3 and Table 3.

The four steps TG of $K_3[Fe(C_2O_4)_3]\cdot 3H_2O$ were optimized. They adopted A → B → C, A → B and C → D, A → B and C → D, A → B → C reaction

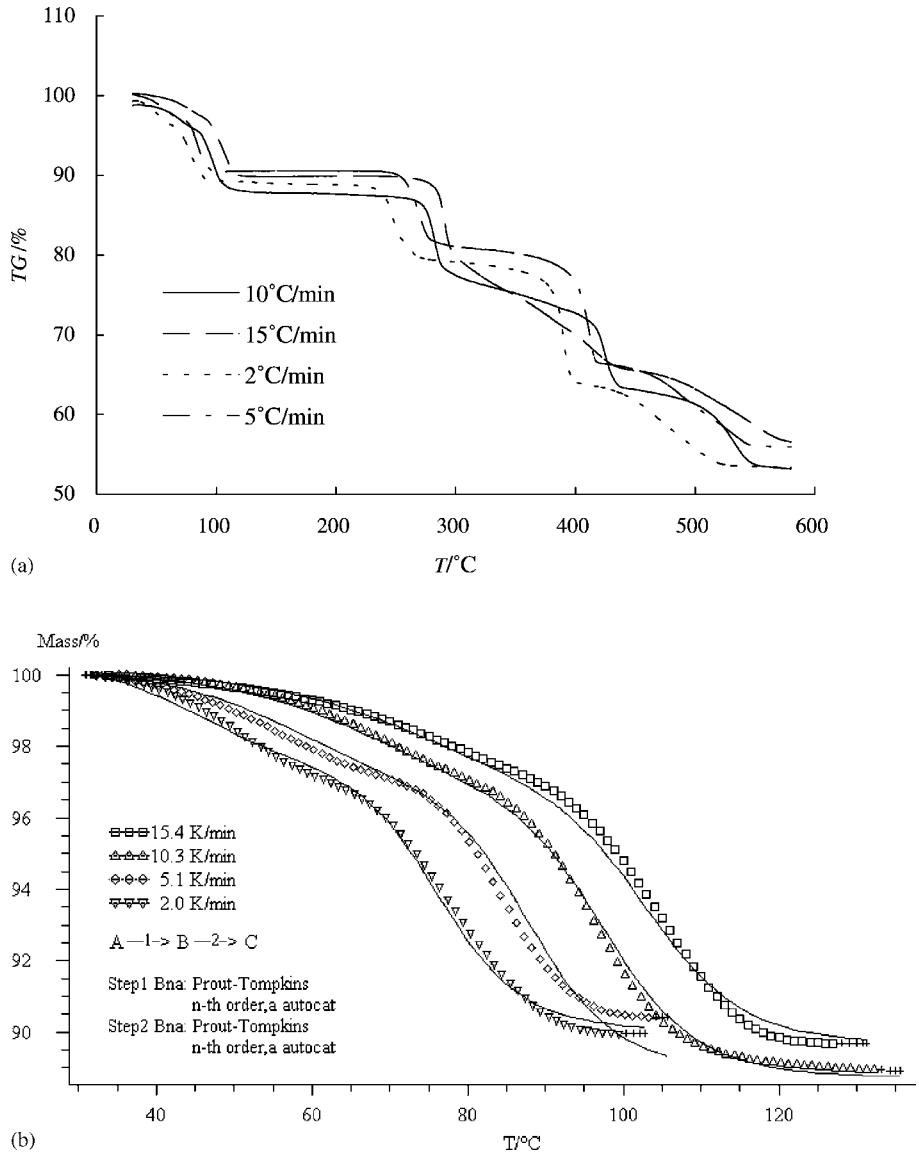

Fig. 3. The TG curve of $K_3Fe(C_2O_4)_3\cdot 3H_2O$ at the heating rate of 15, 10, 5, and 2 °C min^{-1}, respectively (a); the first step (b), the second step (c), the third step (d) and the fourth step (e) were the best fit to mechanism functions. The solid line is the fit curve.

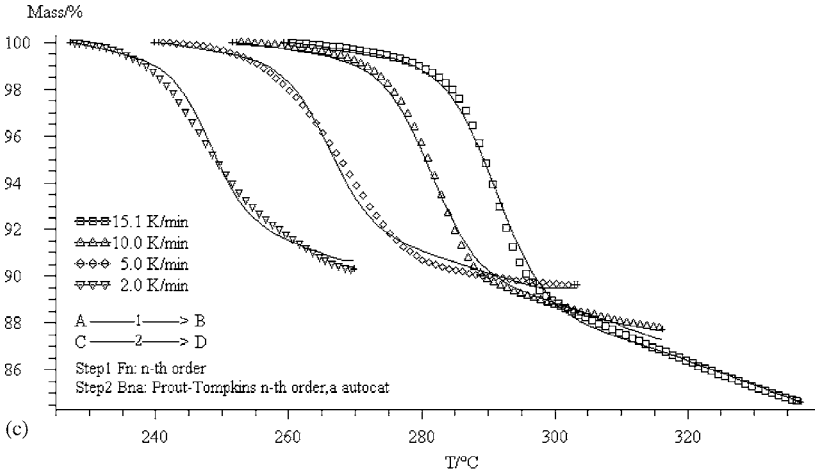

(c)

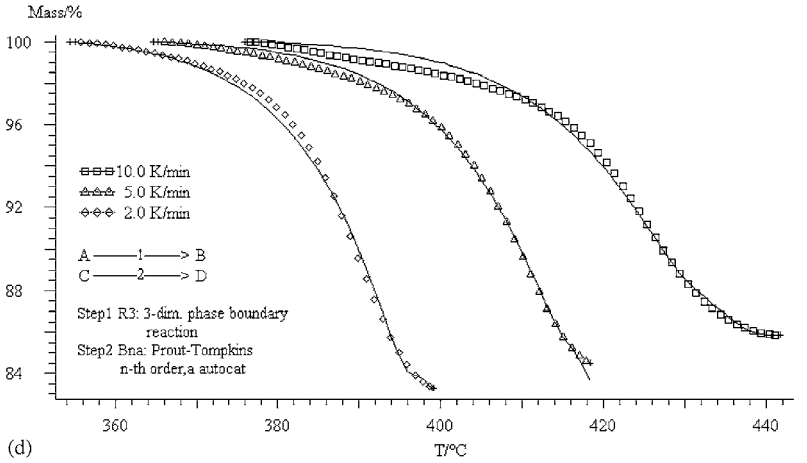

(d)

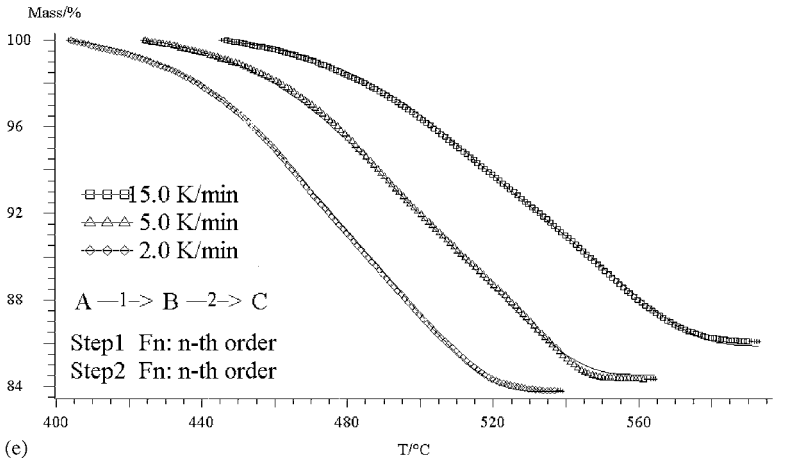

(e)

Fig. 3. (*Continued*).

mode, and the optimized mechanism functions were Bna–Bna, Fn–Bna, R3–Bna and Fn–Fn, respectively. The activation energies of the first and second steps are larger than that of the third and the fourth steps.

3.5. Thermal kinetic TG-analysis of $K_2[Cu(C_2O_4)_2]\cdot 2H_2O$

TG kinetic of the first and the second steps of $K_2[Cu(C_2O_4)_2]\cdot 2H_2O$ were analyzed, respectively. The multireaction mechanism was used to optimize the mechanism function, and the results were shown in Fig. 4 and Table 3.

The results show that the dehydration of $K_2[Cu(C_2O_4)_2]\cdot 2H_2O$ adopted the A → B → C sequential reaction, and the reaction mechanism was Bna–Bna. The second step also adopted A → B → C reaction mode, and the reaction mechanism was A3–D3. Compared with $K_3[Al(C_2O_4)_3]\cdot 3H_2O$ and $K_3[Fe(C_2O_4)_3]\cdot 3H_2O$, the correction coefficient of $K_2[Cu(C_2O_4)_2]\cdot 2H_2O$ is more close to 1.

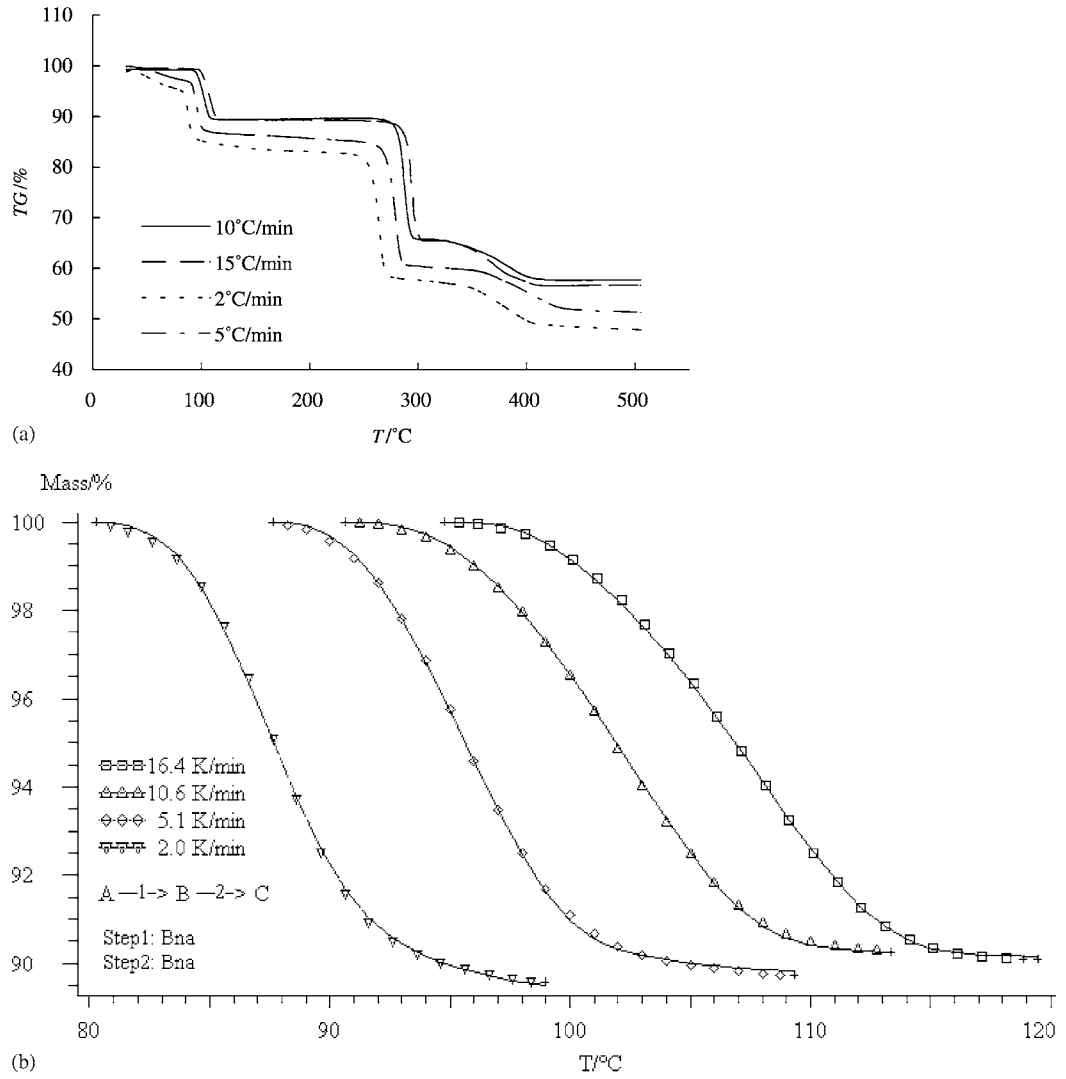

Fig. 4. The TG curve of $K_2Cu(C_2O_4)_2\cdot 2H_2O$ at the heating rate of 15, 10, 5, and 2 °C min^{-1}, respectively (a); the first step (b) and the second step (c) were the best fit to mechanism functions. The solid line is the fit curve.

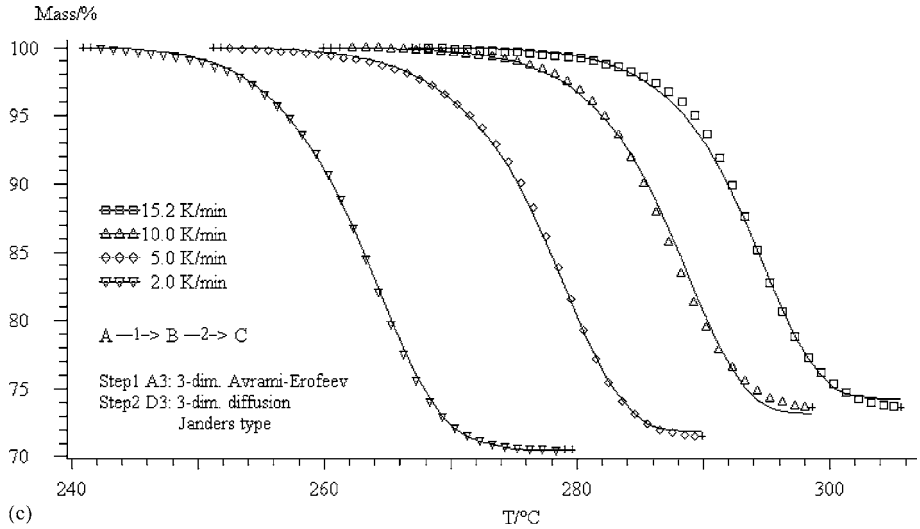

Fig. 4. (*Continued*).

3.6. Discussion

3.6.1. The process of dehydration

The dehydration reaction of $K_3[Al(C_2O_4)_3]\cdot 3H_2O$ undergoes two same chemical reaction mechanisms (Fn) with different E_a, n and $\lg A$ (Table 3) and the later mechanism has the larger activation energy. For $K_3[Cr(C_2O_4)_3]\cdot 3H_2O$, the dehydration mechanism is also formal chemical reaction (Fn) with E_a, n and $\lg A$ being 81.87 kJ mol^{-1}, 1.8, and 9.94 s^{-1}, respectively. Difference from $K_3[Al(C_2O_4)_3]\cdot 3H_2O$ and $K_3[Cr(C_2O_4)_3]\cdot 3H_2O$, the dehydration reaction mechanisms of $K_3[Fe(C_2O_4)_3]\cdot 3H_2O$ and $K_2[Cu(C_2O_4)_2]\cdot 2H_2O$ are auto-catalysis (Bna) and both also undergo two processes with different E_a, n, a and $\lg A$ (Table 3). These can be explained by that the dehydration reactions start on some local place, such as on the crystal lacuna. Subsequently, these dehydration products get together and form a new nuclear. Later, the new nuclear occur phase boundary reaction, and the reactant graduate away and the products grow until the reaction accomplish.

3.6.2. Mechanism functions and activation energies

Analyzing the mechanism functions and activation energies of each steps, we see that auto-catalysis (Bna) corresponds to the smallest activation energies, formal chemical reaction (Fn) takes second place, and three-dimensional nucleation and growth (A3) takes the third, phase boundary reaction contracting sphere (R3) and diffusion three-dimensional diffusion (D3) have the largest activation energies.

4. Evaluation of models

The multireactions mechanism and single reaction mechanism have been used to optimized for each step of these complexes. The results show that the multireactions mechanism are better than single reaction mechanism for $K_3[Al(C_2O_4)_3]\cdot 3H_2O$, $K_3[Fe(C_2O_4)_3]\cdot 3H_2O$ and $K_2[Cu(C_2O_4)_2]\cdot 2H_2O$. We suppose there may exist two or even more reaction mechanisms in a step of thermal decomposition of solids. Of course, some times the parameters gained from optimizing were not good, such as reaction order.

Acknowledgements

We are very grateful for the financial support from The National Natural Science Foundation of China and The National Science Foundation of Shaanxi Province.

References

[1] K.V. Krishnamurty, G.M. Harris, Chem. Rev. 61 (1961) 213.
[2] B.V. L'vov, Thermochim. Acta 373 (2) (2001) 97.
[3] W.W. Wendlandt, T.D. George, J. Inorg. Chem. 21 (1961) 69.
[4] E.L. Simmons, W.W. Wendlandt, J. Inorg. Nucl. Chem. 27 (1965) 2325.
[5] D. Broadbent, D. Dollimore, J. Dollimore, J. Chem. Soc. (1967) 451.
[6] A.S. Brar, B.S. Randhawa, J. Solid State Chem. 58 (1985) 153.
[7] K. Nagase, Bull. Chem. Soc. Jpn. 46 (1973) 144.
[8] N. Deb, S.D. Baruah, N. Sen Sarma, N.N. Dass, Thermochim. Acta 320 (1998) 53.
[9] N. Deb, S.D. Baruah, N.N. Dass, Thermochim. Acta 326 (1999) 43.
[10] N. Deb, Thermochim. Acta 338 (1999) 27.
[11] T. Kebede, K.V. Ramana, M.S. Prasada Rao, Thermochim. Acta 371 (2001) 163.
[12] J. Li, F.-X. Zhang, Y.-F. Nan, in: Q.Z. Shi (Ed.), Thermoanalysis Kinetics and Thermokinetics, Shaanxi Science and Technology Press, Xi'an, 2001, pp. 148–153 (in Chinese).
[13] Chemical Society of Japan (Ed.), A Synthesis Handbook of Inorganic Compounds, Chemistry Industry Press, Peking, 1998, p. 368 (in Chinese).